Applied Mathematical Modelling 71 (2019) 208–222

Contents lists available at ScienceDirect

Applied Mathematical Modelling

journal homepage: www.elsevier.com/locate/apm

A singular element based on dual interpolation BFM for V-shaped notches

Jianming Zhang*, Yunqiao Dong, Weicheng Lin, Chuanming Ju

State Key Laboratory of Advanced Design and Manufacturing for Vehicle Body, College of Mechanical and Vehicle Engineering, Hunan University, Changsha 410082, China

ARTICLE INFO

Article history:
Received 31 January 2018
Revised 4 February 2019
Accepted 13 February 2019
Available online 22 February 2019

Keywords:
V-shaped notch
singular element
stress intensity factor (SIF)
dual interpolation
boundary face method (BFM)

ABSTRACT

A singular element based on dual interpolation boundary face method (DiBFM) is presented for solving V-shaped notch problems in this paper. The stress field around sharp notches is singular, and the singularity orders vary with the notch angle. Thus an element with usual shape functions or traditional singular element cannot lead to high accurate results. To accurately model the distribution of displacement around the notch tip, a new displacement singular element based on DiBFM is proposed. The new element takes into account the variable singularity orders at the notch tip. The dual interpolation method which combines conventional polynomial element interpolation and moving least-squares approximation can provide much higher accuracy than traditional interpolation method. With the proposed singular element based on DiBFM, more accurate displacement results in the vicinity of the notch tip can be evaluated, thus more accurate stress intensity factor (SIF) of the V-shaped notches can be obtained. Numerical examples have demonstrated the validity and accuracy of our method.

1. Introduction

V-notched structures such as gears, bolts and nuts widely appear in the practical engineering problem. These structures are of major interest in engineering design because the failures usually happen in these regions. The stresses at the notch tip are singular. Therefore, accurate and efficient numerical analysis of structures with V-shaped notches has been a challenging task.

The finite element method (FEM) is a successful tool to analyze the engineering problem. But the boundary element method (BEM) [1-14] is more suitable for solving the V-shaped notch problems. In the BEM analysis, only the surface of a body needs to be discretized and accurate results for stress can be obtained. In addition, the trial functions in the FEM formulation must be at least C^0-continuous which is not required in the BEM.

Rzasnicki et al. [15] analyzed single edge notch under pure bending by the BEM. Portela et al. [16] proposed a boundary element singularity subtraction technique to solve the 2D V-shaped notch problems. Niu [17] and Cheng [18] presented an interpolating matrix method to obtain the stresses and the singularity orders of the V-shaped notches. Zhang et al. [19] proposed a singular element based on conventional BEM to compute the stress intensity factor (SIF) of the V-notches.

The boundary face method (BFM) [5-7] is similar to the BEM. Both of them are based on the boundary integral equation. By directly using the boundary representation (B-rep) data structure in most CAD software, no geometric error will be

* Corresponding author.
E-mail address: zhangjm@hnu.edu.cn (J. Zhang).

https://doi.org/10.1016/j.apm.2019.02.020
0307-904X/

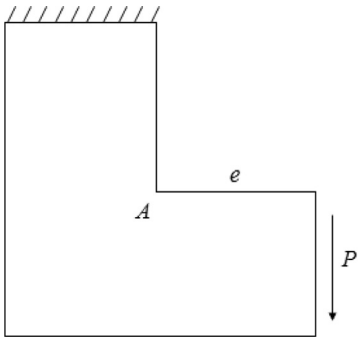

Fig. 1. Structure with V-shaped notch under mixed-mode load.

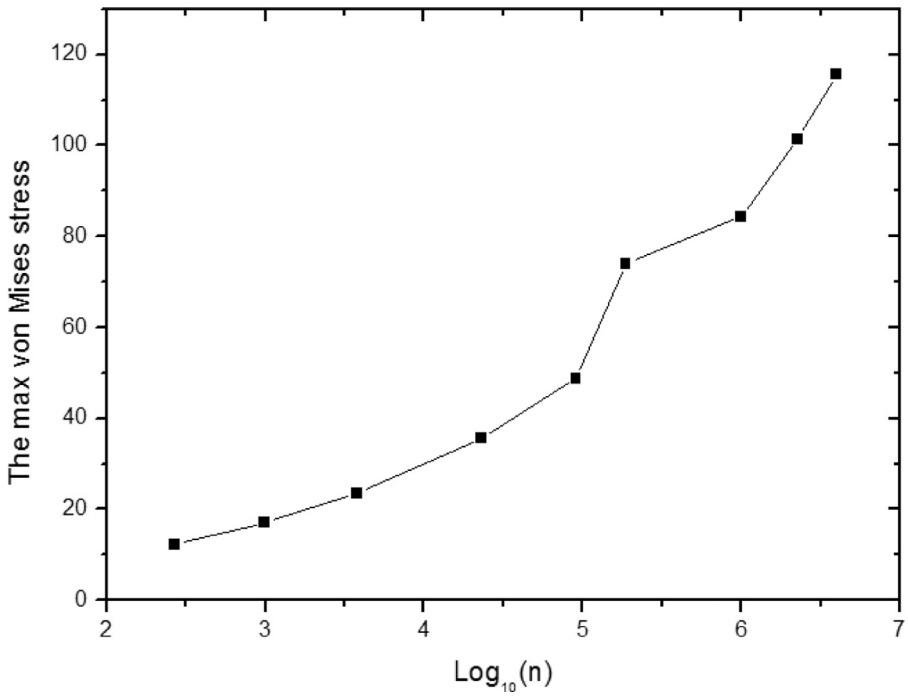

Fig. 2. Von Mises stress obtained by the FEM at point *A*.

introduced in the BFM. Recently, Zhang [1,20,21] has proposed dual interpolation method (DIM) to improve the performance of the BFM. The DIM combines conventional polynomial element interpolation and moving least-squares approximation. The element of DIM is obtained by adding virtual nodes to a conventional discontinuous element at the vertices and edges of a geometric element. The interpolation accuracy of the DIM element will increase by two orders compared with the corresponding discontinuous element. Both continuous and discontinuous fields can be accurately approximated. The DiBFM provides higher accuracy than the traditional BFM.

The stress singularity orders vary with the notch angle. Thus an element with usual shape functions which allow for polynomial variation only is not suitable for modelling the displacement field around the notch tip. The traditional crack tip element [22,23] is also invalid due to the variable singularity orders at the notch tip. Thus a new singular element based on DiBFM is proposed in this paper.

The stresses have several orders of the singularity. The dominant singularity mainly depends on eigenvalue λ_1. Thus, the $r^{\lambda 1}$ variation is incorporated into the proposed element. λ_1 is a function with respect to the notch angle. To make full use of the DiBFM, the special shape functions of the proposed element are derived within DiBFM. With the proposed singular element based on the DiBFM, more accurate displacement results in the vicinity of the notch tip can be evaluated, thus more accurate SIF of the V-shaped notches can be obtained.

The paper is outlined as follows. The FEM for the V-shaped notch problem is presented in Section 2. The element of dual interpolation method is introduced in Section 3. Section 4 describes the proposed element based on DiBFM. Four numerical examples are shown in Section 5. The conclusion is given in Section 6.

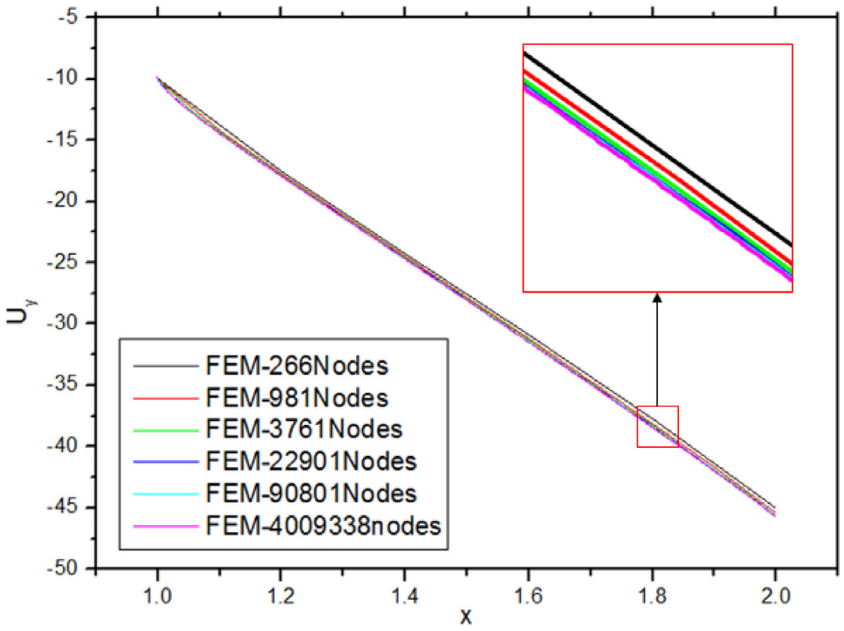

Fig. 3. Displacements along edge e by the FEM with different number of nodes.

2. The finite element method for the V-shaped notch problem

A structure with V-shaped notch is under mixed-mode load (Fig. 1). The von Mises stress obtained by the FEM with different number of mesh node at point A is shown in Fig. 2. It can be seen that von Mises stress does not converge and grow up rapidly with increasing number of mesh nodes (n). This illustrates that evaluating stress at singular point is meaningless. The fracture criterion of the V-shaped notch should be dependent on the SIF.

Although stresses at the tip point of a notch do not converge, theoretically the displacements at it obtained by the FEM can be convergent. Fig. 3 shows an FEM results for displacements along the edge e with different number of nodes. One can see that as the number of the mesh nodes increase, the results keep almost unchanging. Therefore, a numerical result by FEM for displacements with a large number of elements can be used a reference "exact" solution for comparison. Accordingly, in this paper we will make use of this point to validate our method.

3. Element of dual interpolation method

In this section, the element of dual interpolation method (DIM) is briefly introduced. The DIM element is obtained by adding virtual nodes to a conventional discontinuous element at the vertices of a geometric element. Fig. 4 shows a quadratic DIM element. Considering the virtual nodes and source nodes, the DIM element becomes a continuous element. According to the positions of the virtual nodes and source nodes, the shape functions can be obtained using Lagrange interpolating polynomial. The shape functions of the quadratic DIM element are given by

$$\begin{cases} N_1 = \dfrac{[\xi+(1-d)][\xi-(1-d)](\xi-1)\xi}{2d(2-d)} \\ N_2 = \dfrac{[\xi+(1-d)][\xi-(1-d)](\xi+1)\xi}{2d(2-d)} \\ N_3 = -\dfrac{[\xi-(1-d)](\xi+1)(\xi-1)\xi}{2d(2-d)(1-d)^2} \\ N_4 = -\dfrac{[\xi+(1-d)](\xi+1)(\xi-1)\xi}{2d(2-d)(1-d)^2} \\ N_5 = \dfrac{[\xi+(1-d)][\xi-(1-d)](\xi+1)(\xi-1)}{(1-d)^2} \end{cases} \tag{1}$$

where $\xi \in [-1, 1]$ is the natural coordinate of the element. d denotes the offset of source nodes, and $d = 0.25$ in this paper. From Eq. (1), one can see that the interpolation accuracy of the DIM element increases by two orders compared with the original quadratic discontinuous element.

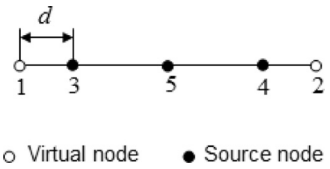

Fig. 4. A quadratic DIM element.

The DIM element is used for interpolating boundary variables. The boundary integral equation is collocated at the source node, only. The moving least-squares (MLS) approximation is used to construct relationships between variables on source nodes and virtual nodes. The DIM combines conventional polynomial element interpolation and moving least-squares approximation. Both continuous and discontinuous fields can be accurately approximated. The DiBFM provides higher accuracy than the traditional BFM.

4. New singular element based on DiBFM

We first introduce singularity orders of V-notch in this section. Then the shape functions of the proposed element based on DiBFM are derived in detail.

4.1. Singularity orders of V-notch

The stresses in the vicinity of the notch tip are [24]

$$\sigma_r = \frac{S_{\mathrm{I}}}{\sqrt{2\pi}(r)^{1-\lambda_1}}\left\{-\cos(1+\lambda_1)\theta - \frac{(3-\lambda_1)\sin(1+\lambda_1)\alpha}{(1-\lambda_1)\sin(1-\lambda_1)\alpha}\cos(1-\lambda_1)\theta\right\} + \frac{S_{\mathrm{II}}}{\sqrt{2\pi}(r)^{1-\lambda_2}}\left\{\sin(1+\lambda_2)\theta + \frac{(3-\lambda_2)\sin(1+\lambda_2)\alpha}{(1+\lambda_2)\sin(1-\lambda_2)\alpha}\sin(1-\lambda_2)\theta\right\} \tag{2}$$

$$\sigma_\theta = \frac{S_{\mathrm{I}}}{\sqrt{2\pi}(r)^{1-\lambda_1}}\left\{\cos(1+\lambda_1)\theta - \frac{(1+\lambda_1)\sin(1+\lambda_1)\alpha}{(1-\lambda_1)\sin(1-\lambda_1)\alpha}\cos(1-\lambda_1)\theta\right\} + \frac{S_{\mathrm{II}}}{\sqrt{2\pi}(r)^{1-\lambda_2}}\left\{\sin(1+\lambda_2)\theta + \frac{\sin(1+\lambda_2)\alpha}{\sin(1-\lambda_2)\alpha}\sin(1-\lambda_2)\theta\right\} \tag{3}$$

and

$$\sigma_{r\theta} = \frac{S_{\mathrm{I}}}{\sqrt{2\pi}(r)^{1-\lambda_1}}\left\{\sin(1+\lambda_1)\theta - \frac{\sin(1+\lambda_1)\alpha}{\sin(1-\lambda_1)\alpha}\sin(1-\lambda_1)\theta\right\} + \frac{S_{\mathrm{II}}}{\sqrt{2\pi}(r)^{1-\lambda_2}}\left\{\cos(1+\lambda_2)\theta - \frac{(1-\lambda_2)\sin(1+\lambda_2)\alpha}{(1+\lambda_2)\sin(1-\lambda_2)\alpha}\cos(1-\lambda_2)\theta\right\} \tag{4}$$

The associated displacements are given by [24]

$$u_r = \frac{S_I(r)^{\lambda_1}}{\sqrt{2\pi}G}\left\{-\frac{1}{2\lambda_1}\cos(1+\lambda_1)\theta + \frac{\sin(1+\lambda_1)\alpha}{(1-\lambda_1)(1-t)\sin(1-\lambda_1)\alpha}\cos(1-\lambda_1)\theta\right\} + \frac{S_{II}(r)^{\lambda_2}}{\sqrt{2\pi}G}\left\{-\frac{1}{2\lambda_2}\sin(1+\lambda_2)\theta + \frac{\sin(1+\lambda_2)\alpha}{(1+\lambda_2)(1-t)\sin(1-\lambda_2)\alpha}\sin(1-\lambda_2)\theta\right\} \tag{5}$$

and

$$u_\theta = \frac{S_{\mathrm{I}}(r)^{\lambda_1}}{\sqrt{2\pi}G}\left\{\frac{1}{2\lambda_1}\sin(1+\lambda_1)\theta - \frac{t\sin(1+\lambda_1)\alpha}{(1-\lambda_1)(1-t)\sin(1-\lambda_1)\alpha}\sin(1-\lambda_1)\theta\right\} + \frac{S_{\mathrm{II}}(r)^{\lambda_2}}{\sqrt{2\pi}G}\left\{-\frac{1}{2\lambda_2}\cos(1+\lambda_2)\theta + \frac{t\sin(1+\lambda_2)\alpha}{(1+\lambda_2)(1-t)\sin(1-\lambda_2)\alpha}\cos(1-\lambda_2)\theta\right\} \tag{6}$$

where r and θ denote the polar radius and polar angle respectively in polar coordinate system as shown in Fig. 5; G is the shear modulus; The notch angle equals to 2β and angle α equals to $\pi-\beta$; Eigenvalues λ_1 and λ_2 can be obtained by the following equations:

$$\lambda_1\sin(2\alpha) + \sin(2\lambda_1\alpha) = 0 \tag{7}$$

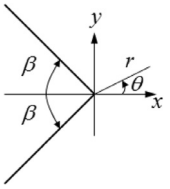

Fig. 5. A V-notch.

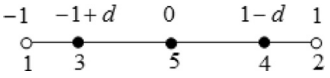

Fig. 6. The proposed element.

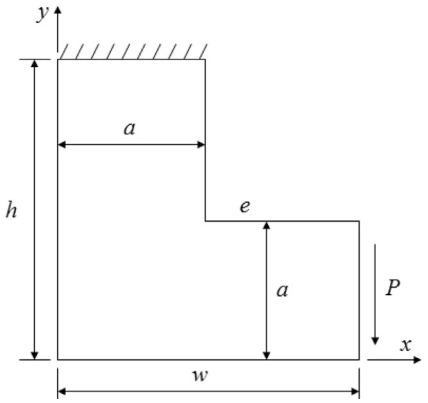

Fig. 7. A V-notch subjected to mixed-mode load.

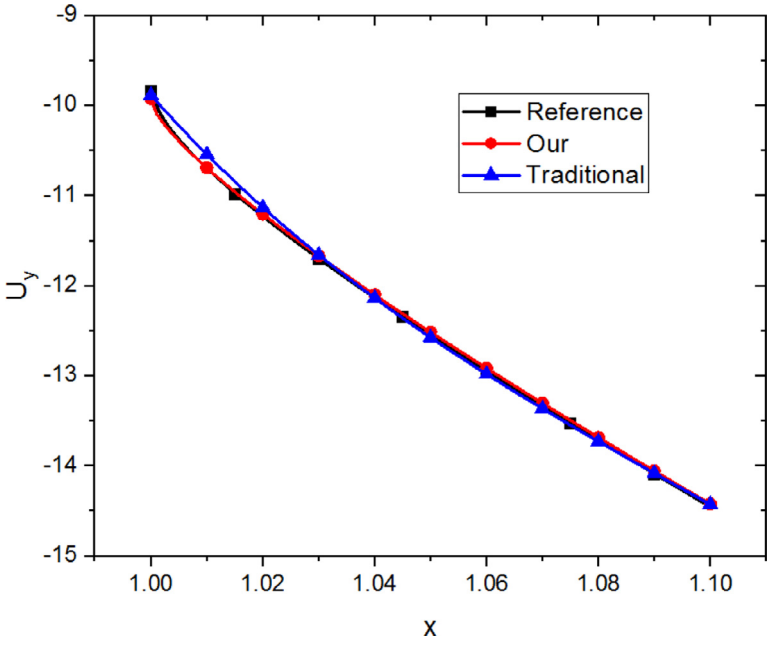

Fig. 8. Displacement U_y along the edge e.

$$\lambda_2 \sin(2\alpha) - \sin(2\lambda_2\alpha) = 0 \tag{8}$$

The SIFs are computed by

$$K_{\mathrm{I}} = \lim_{r\to 0} \sqrt{2\pi}\,(r)^{1-\lambda_1}\sigma_\theta|_{\theta=0} \tag{9}$$

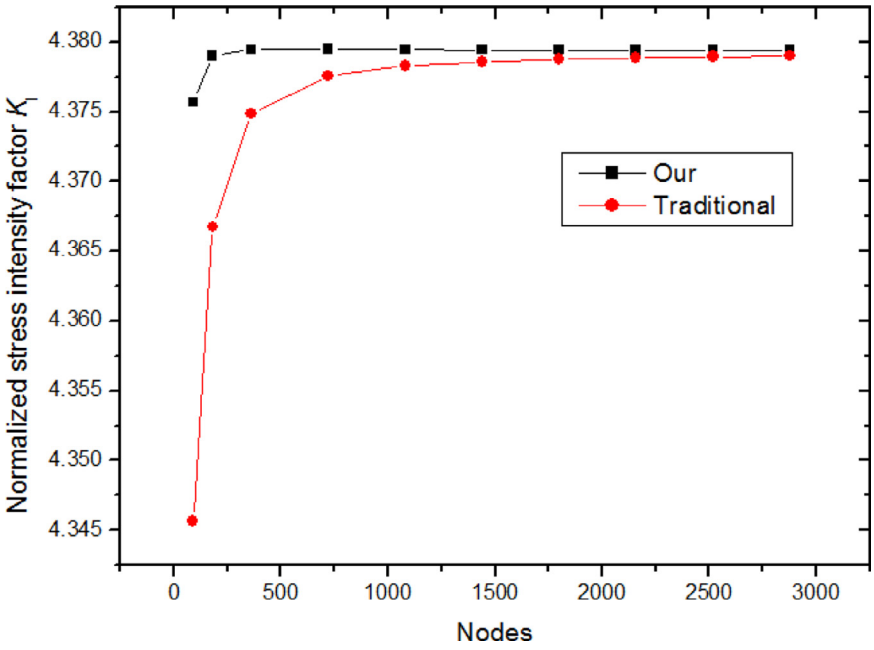

Fig. 9. Normalized SIF $K_I/P\sqrt{\pi a}$.

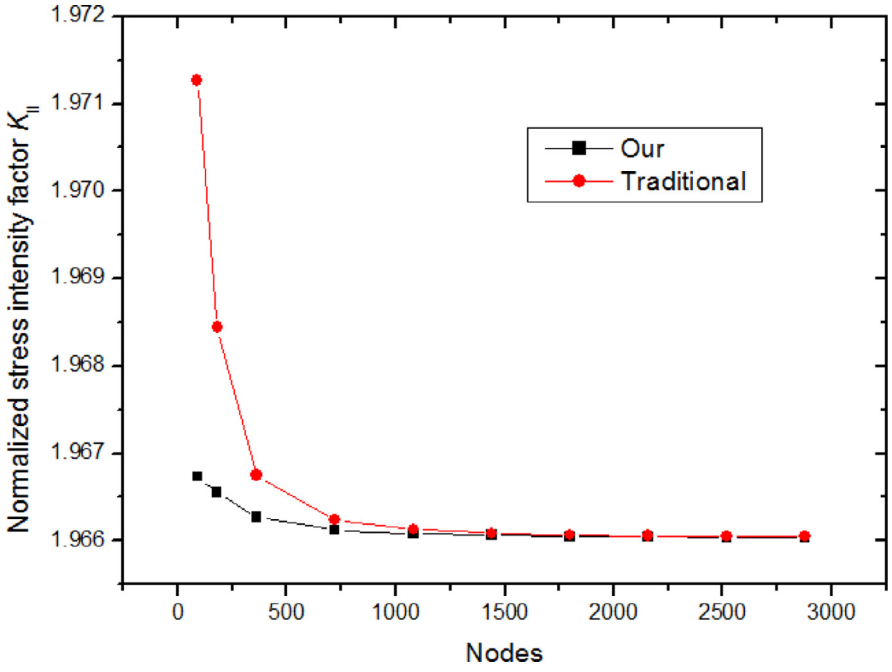

Fig. 10. Normalized SIF $K_{II}/P\sqrt{\pi a}$.

$$K_{II} = \lim_{r\to 0} \sqrt{2\pi}\,(r)^{1-\lambda_2}\sigma_{r\theta}|_{\theta=0} \tag{10}$$

4.2. Shape functions of the proposed element

From Eqs. (2)–(8), one can see that the dominant singularity mainly depends on eigenvalue λ_1. Thus, the $r^{\lambda 1}$ variation is incorporated into the proposed element.

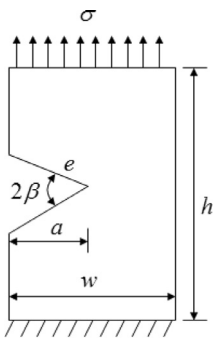

Fig. 11. Single edge V-notch plate subjected to tension load.

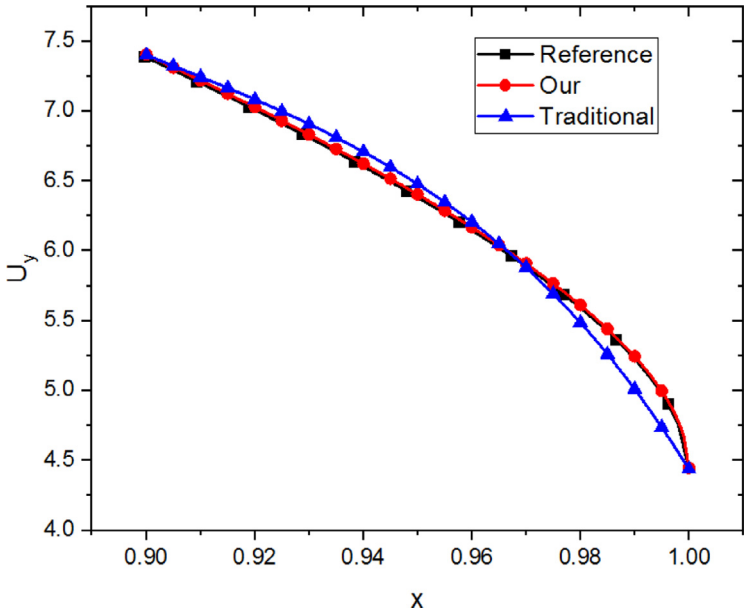

Fig. 12. Displacement U_y along the edge e when $2\beta = \pi/6$.

The proposed element as shown in Fig. 6 is based on the quadratic DIM element. Assuming that the node 1 of the singular element lies at notch tip, to get the desired variation, the shape functions of the proposed element should be of the following form:

$$N^i = a_0^i + a_1^i(1+\xi)^{\lambda_1} + a_2^i(1+\xi)^{2\lambda_1} + a_3^i(1+\xi)^{3\lambda_1} + a_4^i(1+\xi)^{4\lambda_1} \tag{11}$$

where $i = 0,\ldots, 4$; N^i represents the ith special shape function; $a_0^i \sim a_4^i$ are undetermined coefficients.

Eq. (11) should satisfy the following condition:

$$N^i(\xi_j) = \delta_{ij} \tag{12}$$

where $i, j = 0,\ldots, 4$; δ_{ij} is Kronecker delta function; ξ_j is the local node coordinate of the proposed element (Fig. 6).

Solving above linear system of equations will get the undetermined coefficients $a_0^i \sim a_4^i$. With the proposed singular element based on the DiBFM, more accurate displacement results in the vicinity of the notch tip can be evaluated, thus more accurate SIF of the V-shaped notches can be obtained.

5. Numerical examples

To verify the validity and accuracy of the proposed element, four examples are presented in this section.

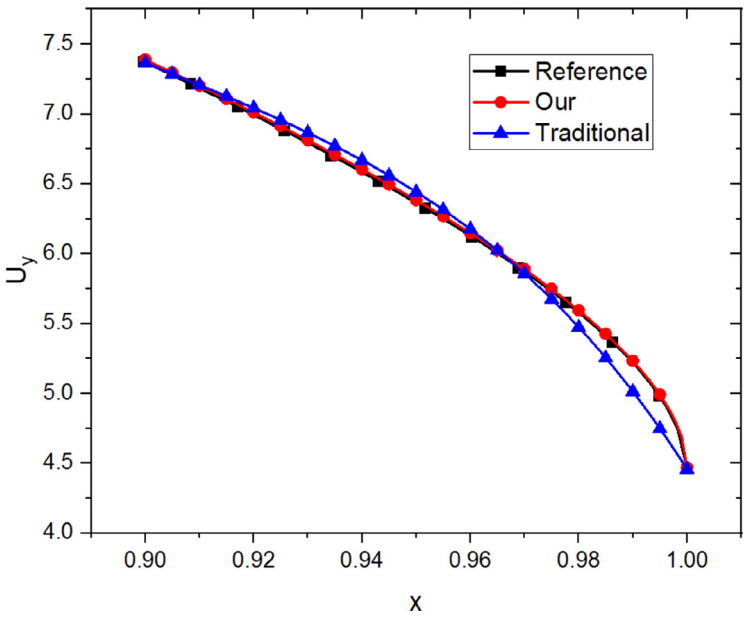

Fig. 13. Displacement U_y along the edge e when $2\beta = \pi/3$.

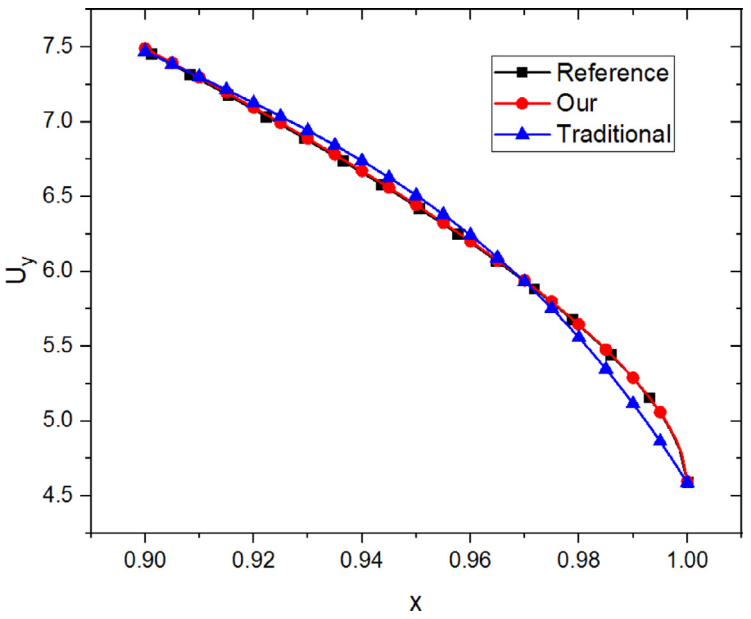

Fig. 14. Displacement U_y along the edge e when $2\beta = \pi/2$.

5.1. Example 1: V-notch subjected to mixed-mode load

In the first example, we consider a V-notch subjected to mixed-mode load (Fig. 7). Young's modulus is 1 (in consistent units) and Poisson's ratio is 0.25. The geometric parameters h/w and a/w are 1 and 0.5, respectively. Plane strain cases are concerned.

The displacement U_y along the edge e are shown in Fig. 8. 'Reference' represents the results obtained by the FEM software ABAQUS with 4,009,338 mesh nodes. 'Our' stands for the results obtained by the proposed method. 'Traditional' is the results obtained by the traditional DiBFM with usual element. 90 nodes are used in these two methods. It can be seen that high accurate displacement U_y can be obtained by our method.

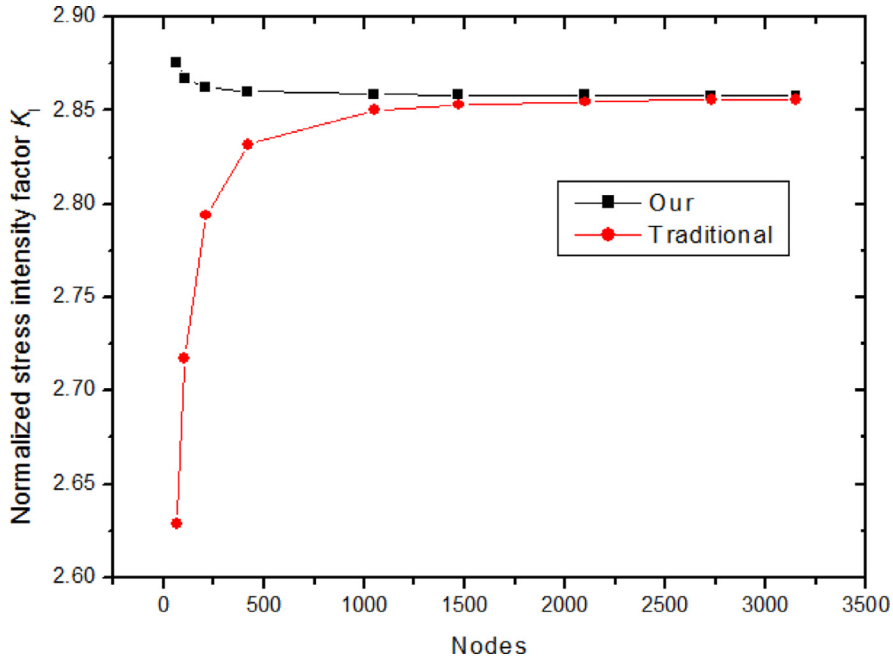

Fig. 15. Normalized SIF $K_I/\sigma\sqrt{\pi a}$ when $2\beta=\pi/6$.

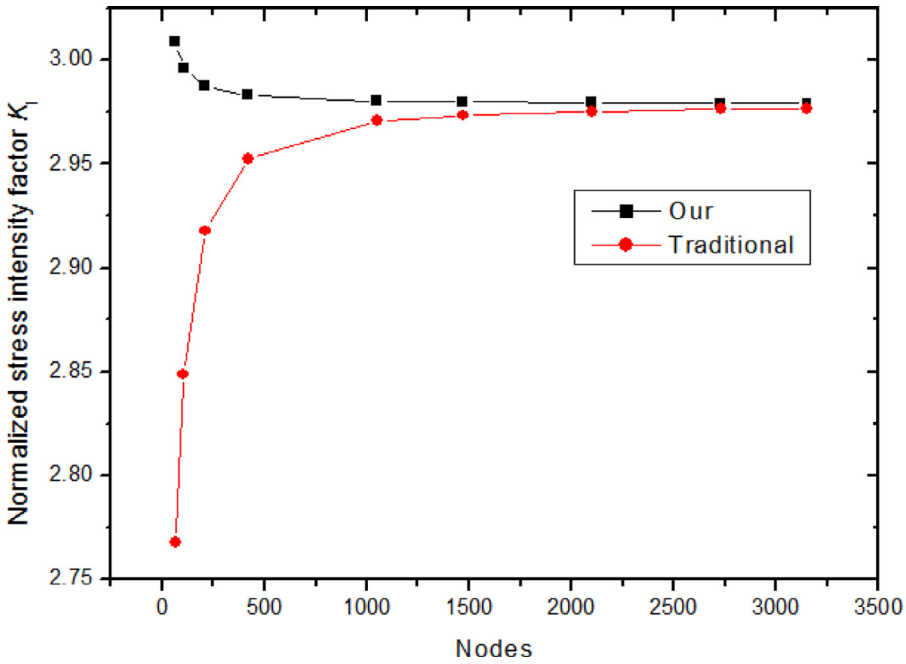

Fig. 16. Normalized SIF $K_I/\sigma\sqrt{\pi a}$ when $2\beta=\pi/3$.

Figs. 9 and 10 show the normalized SIFs $K_I/P\sqrt{\pi a}$ and $K_{II}/P\sqrt{\pi a}$ by different number of nodes, respectively. As illustrated in these two figures that the results for SIFs are convergent with increasing of nodes, and the SIFs obtained by our method get closer to the convergence solution compared with those by the traditional DiBFM when using few nodes.

5.2. Example 2: single edge V-notch subjected to tension load

A single edge V-notch is considered in this case. Young's modulus is 1 (in consistent units) and Poisson's ratio is 0.25. The geometric parameters h/w and a/w are 1.75 and 0.5, respectively. The notch angle $2\beta=\pi/6$, $\pi/3$ and $\pi/2$. Plane strain cases are concerned. The V-notched plate is subjected to tension load σ as shown in Fig. 11.

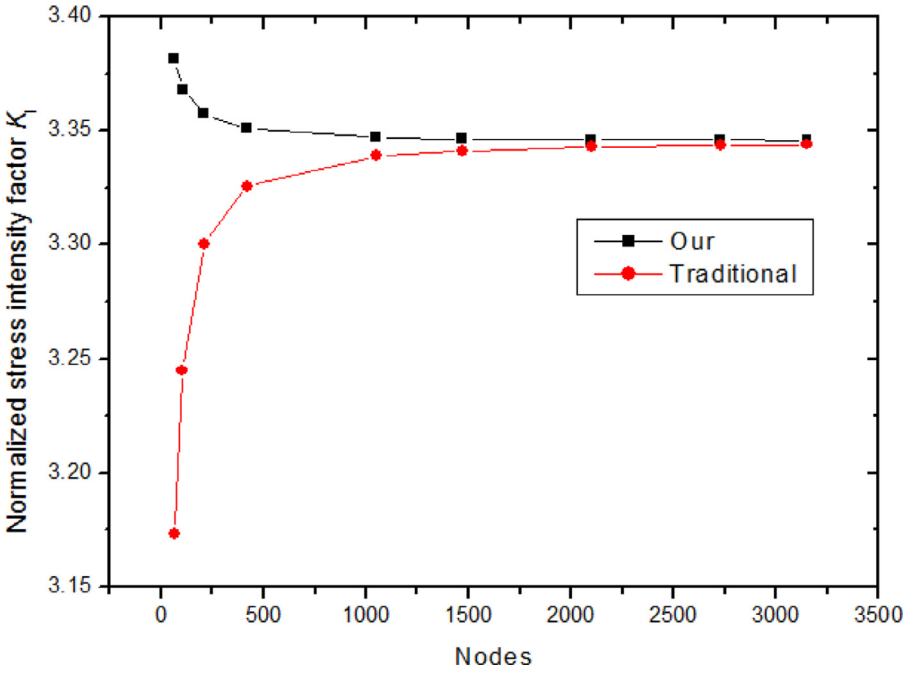

Fig. 17. Normalized SIF $K_I/\sigma\sqrt{\pi a}$ when $2\beta=\pi/2$.

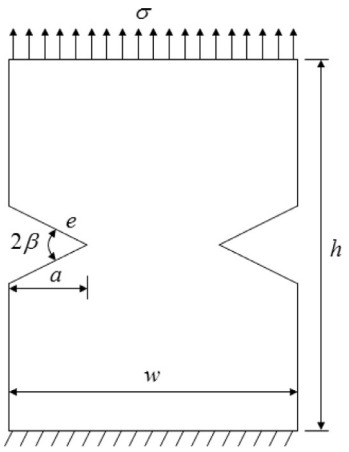

Fig. 18. Double edge V-notch plate subjected to tension load.

Figs. 12–14 show the displacement U_y along the edge e when $2\beta=\pi/6$, $\pi/3$ and $\pi/2$, respectively. 'Reference' represents the results obtained by the FEM software ABAQUS with more than 5 million mesh nodes. 'Our' stands for the results obtained by the proposed method. 'Traditional' is the results obtained by the traditional DiBFM with usual element. 105 nodes are used in these two methods. It can be seen that high accurate displacement U_y can be obtained by our method.

Figs. 15–17 show the normalized SIF $K_I/\sigma\sqrt{\pi a}$ for different notch angle $2\beta=\pi/6$, $\pi/3$ and $\pi/2$, respectively. As illustrated in these three figures that the results for SIF are convergent with increasing of nodes, and the SIFs obtained by our method get closer to the convergence solution compared with those by the traditional DiBFM when using few nodes.

5.3. Example 3: double edge V-notch subjected to tension load

A double edge V-notch is considered in this example. Young's modulus is 1 (in consistent units) and Poisson's ratio is 0.25. The geometric parameters h/w and a/w are 2 and 0.5, respectively. The notch angle $2\beta=\pi/6$, $\pi/3$ and $\pi/2$. Plane strain cases are concerned. The V-notched plate is subjected to tension load σ as shown in Fig. 18.

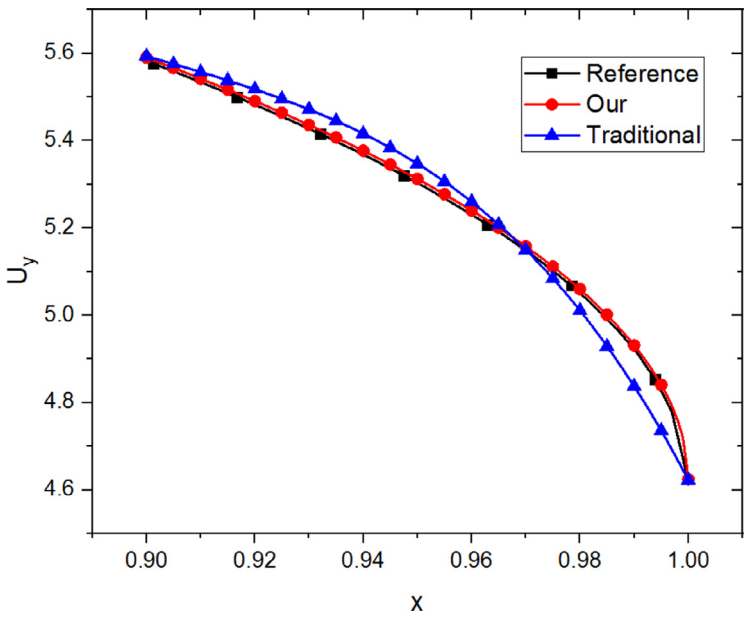

Fig. 19. Displacement U_y along the edge e when $2\beta = \pi/6$.

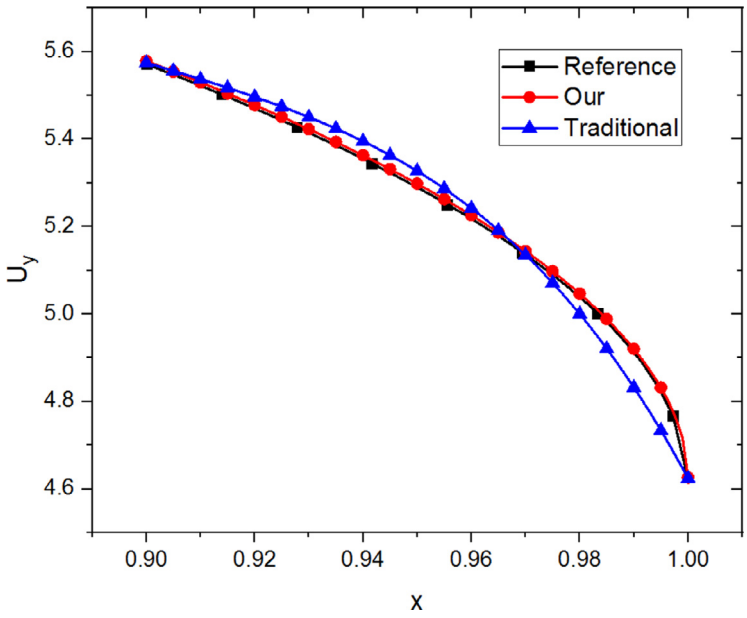

Fig. 20. Displacement U_y along the edge e when $2\beta = \pi/3$.

Figs. 19–21 show the displacement U_y along the edge e when $2\beta = \pi/6$, $\pi/3$ and $\pi/2$, respectively. 'Reference' represents the results obtained by the FEM software ABAQUS with more than 5 million mesh nodes. 'Our' stands for the results obtained by the proposed method. 'Traditional' is the results obtained by the traditional DiBFM with usual element. 150 nodes are used in these two methods. It can be seen that high accurate displacement U_y can be obtained by our method.

Figs. 22–24 show the normalized SIF $K_I/\sigma\sqrt{\pi a}$ for different notch angle $2\beta = \pi/6$, $\pi/3$ and $\pi/2$, respectively. As illustrated in these three figures that the results for SIF are convergent with increasing of nodes, and the SIFs obtained by our method get closer to the convergence solution compared with those by the traditional DiBFM when using few nodes.

5.4. Example 4: open spanner with two V-notches

To further demonstrate the effectiveness of the proposed element, an open spanner with two V-notches is presented in this example. Young's modulus is 1 (in consistent units) and Poisson's ratio is 0.25. The geometric parameters φ and l are

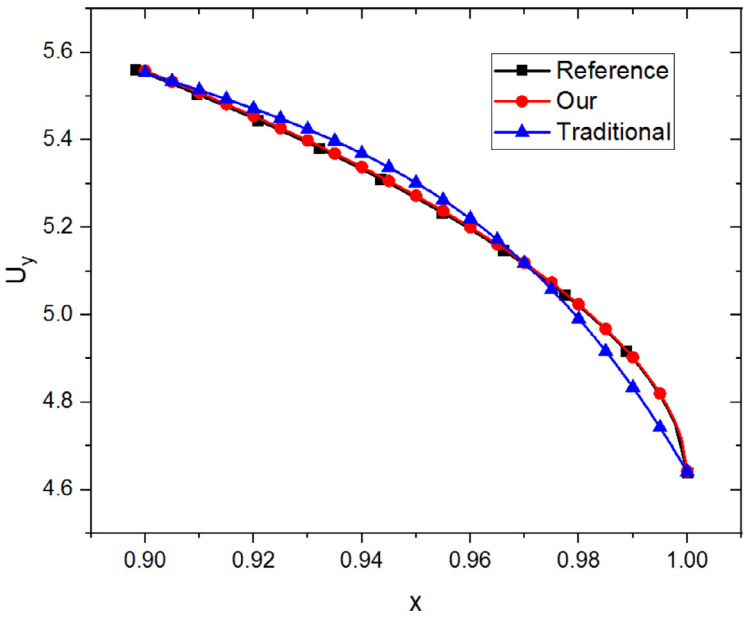

Fig. 21. Displacement U_y along the edge e when $2\beta = \pi/2$.

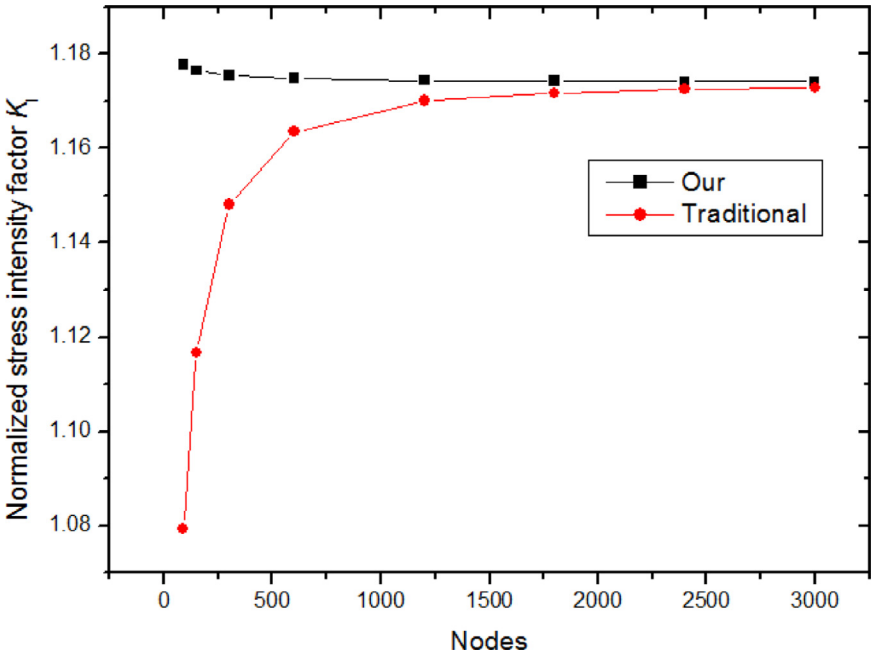

Fig. 22. Normalized SIF $K_I/P\sqrt{\pi a}$ when $2\beta = \pi/6$.

38 and 115, respectively. The traction load P is -1. The displacements along edges b and c are constrained as shown in Fig. 25.

Figs. 26 shows the displacement U_y along the edge e. 'Reference' represents the result obtained by the FEM software ABAQUS with 5,613,540 mesh nodes. 'Our' stands for the result obtained by the proposed method. 'Traditional' is the result obtained by the traditional DiBFM with usual element. 603 nodes are used in these two methods. It can be seen that displacement U_y obtained by the traditional DiBFM is fluctuant around the notch tip. Fig. 27 shows the von Mises stress distribution obtained by the proposed method. These demonstrate that our method is able to solve complicated engineering problem.

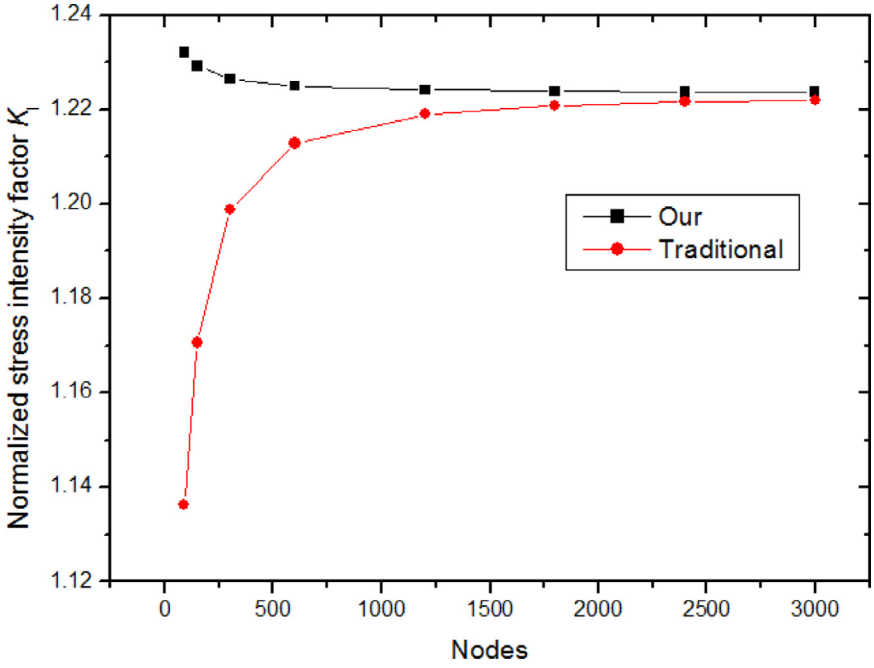

Fig. 23. Normalized SIF $K_I/P\sqrt{\pi a}$ when $2\beta = \pi/3$.

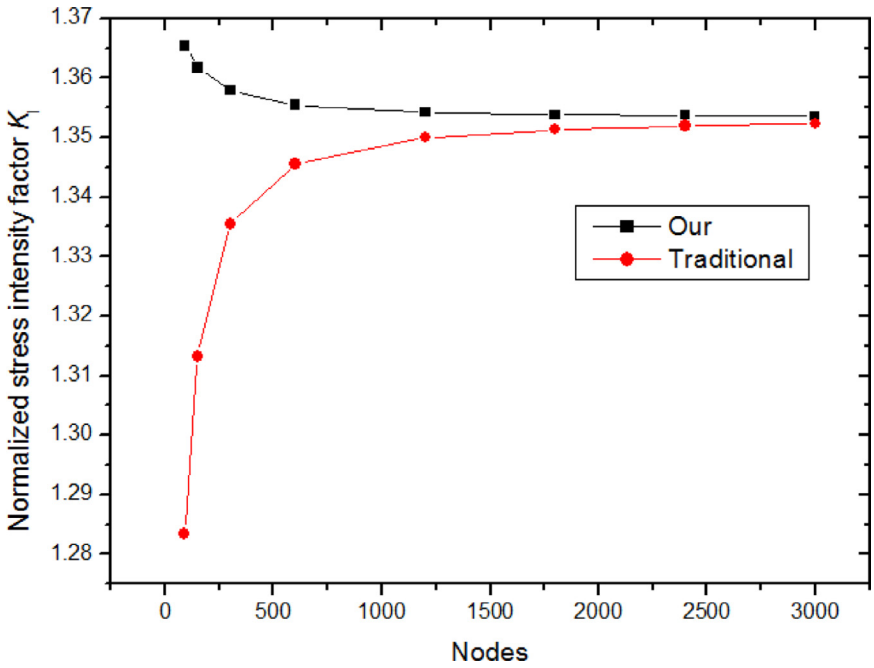

Fig. 24. Normalized SIF $K_I/P\sqrt{\pi a}$ when $2\beta = \pi/2$.

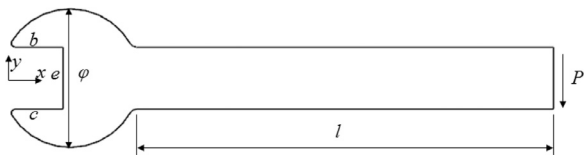

Fig. 25. An open spanner with two V-notches.

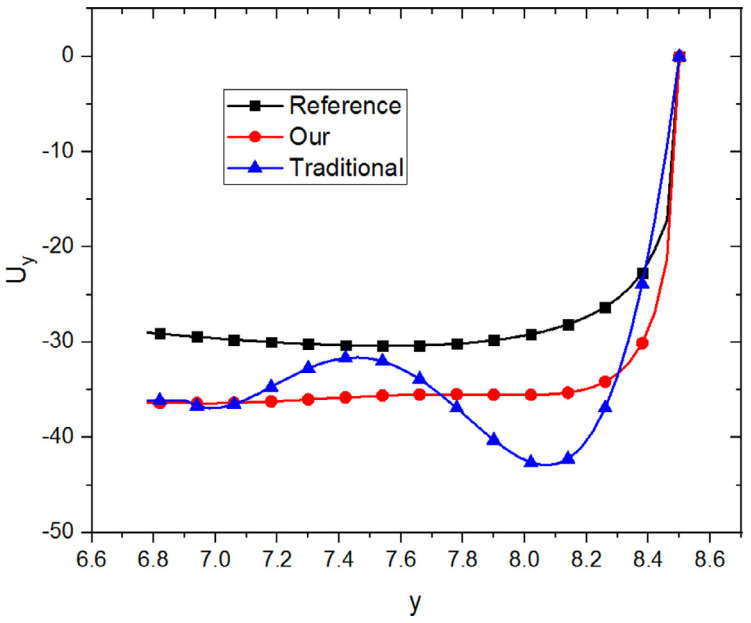

Fig. 26. Displacement U_y along the edge *e*.

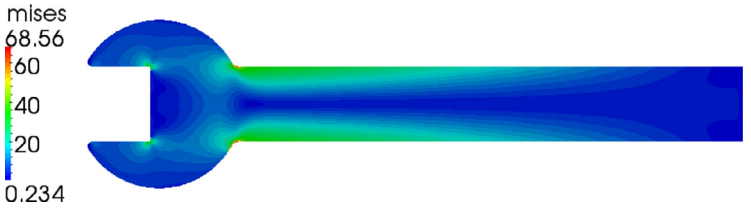

Fig. 27. Von Mises stress distribution.

6. Conclusion

A singular element based on DiBFM is proposed for solving V-shaped notch problems in this paper. The stress field around sharp notches is singular, thus evaluating stress at singular point is meaningless. The fracture criterion of the V-shaped notch should be dependent on the SIF. The new element takes into account the variable singularity orders at the notch tip. The DiBFM can provide much higher accuracy than conventional BFM. Numerical examples have shown that with the proposed singular element based on DiBFM, more accurate results for displacement in the vicinity of the notch tip and SIF of the V-shaped notches can be obtained.

Acknowledgments

This work was supported by National Science Foundation of China under grant numbers 11772125 and 11472102.

References

[1] J.M. Zhang, W.C. Lin, Y.Q. Dong, et al., A double-layer interpolation method for implementation of BEM analysis of problems in potential theory, Appl. Math. Model. 51 (2017) 250–269.
[2] G.Z. Xie, J.M. Zhang, Y.Q. Dong, et al., An improved exponential transformation for nearly singular boundary element integrals in elasticity problems, Int. J. Solids Struct. 51 (6) (2014) 1322–1329.
[3] Y.Q. Dong, J.M. Zhang, G.Z. Xie, et al., A general algorithm for evaluating domain integrals in 2D boundary element method for transient heat conduction, Int. J. Comput. Methods 12 (2) (2015) 1550010. 13 pages.
[4] Y. Li, J.M. Zhang, G.Z. Xie, et al., Time-domain BEM analysis for three-dimensional elastodynamic problems with initial conditions, CMES-Comput. Model. Eng. Sci. 101 (3) (2014) 187–206.
[5] J.M. Zhang, C.J. Lu, Y. Li, et al., A domain renumbering algorithm for multi-domain boundary face method, Eng. Anal. Bound. Elem. 44 (2014) 19–27.
[6] C. Huang, J.M. Zhang, X.Y. Qin, et al., Stress analysis of solids with open-ended tubular holes by BFM, Eng. Anal. Bound. Elem. 36 (2012) 1908–1916.
[7] X.Y. Qin, J.M. Zhang, G.Y. Li, et al., An element implementation of the boundary face method for 3D potential problems, Eng. Anal. Bound. Elem. 34 (2010) 934–943.
[8] J.P. Li, W. Chen, A modified singular boundary method for three-dimensional high frequency acoustic wave problems, Appl. Math. Model. 54 (2018) 189–201.

[9] M.M. Muñoz-Reja, F.C. Buroni, A. Sáez, et al., 3D explicit-BEM fracture analysis for materials with anisotropic multifield coupling, Appl. Math. Model. 40 (4) (2016) 2897–2912.
[10] P. Zhao, T.Y. Qin, L.N Zhang, A regularized time-domain BIEM for transient elastodynamic crack analysis in piezoelectric solids, Eng. Anal. Bound. Elem. 56 (2015) 145–153.
[11] Y.J. Liu, H. Fan, Analysis of the thin piezoelectric solids by the boundary element method, Comput. Methods Appl. Mech. Eng. 191 (2002) 2297–2315.
[12] H. Ma, N. Kamiya, A general algorithm for the numerical evaluation of nearly singular boundary integrals of various orders for two- and three-dimensional elasticity, Comput. Mech. 29 (4) (2002) 277–288.
[13] C.Y. Dong, Z.C. Xie, Z.H. Yao, et al., Some numerical solution methods of hypersingular integrals in BIE, Adv. Mech. 25 (3) (1995) 424–429.
[14] Q.H. Qin, Y.Y. Huang, BEM of postbuckling analysis of thin plates, Appl. Math. Model. 14 (10) (1990) 544–548.
[15] W. Rzasnicki, A Mendelson, Application of boundary integral method to elastoplastic analysis of V-notched beams, Int. J. Fract. 11 (2) (1975) 329–342.
[16] A. Portela, M.H. Aliabadi, D.P Rooke, Efficient boundary element analysis of sharp notched plates, Int. J. Numer. Methods Eng. 32 (3) (1991) 445–470.
[17] Z.R. Niu, C.Z. Cheng, J.Q Ye, et al., A new boundary element approach of modeling singular stress fields of plane V-notch problems, Int. J. Solids Struct. 46 (16) (2009) 2999–3008.
[18] C.Z. Cheng, S.Y. Ge, S.L. Yao, et al., Singularity analysis for a V-notch with angularly inhomogeneous elastic properties, Int. J. Solids Struct. 78 (2016) 138–148.
[19] J.M. Zhang, Y.Q. Dong, C.M. Ju, et al., A new singular element for evaluating stress intensity factors of V-shaped notches under mixed-mode load, Eng. Anal. Bound. Elem. 93 (2018) 161–166.
[20] J.M. Zhang, L. Han, W.C. Lin, et al., A new implementation of BEM by an expanding element interpolation method, Eng. Anal. Bound. Elem. 78 (2017) 1–7.
[21] J.M. Zhang, Y.D. Zhong, Y.Q. Dong, et al., Expanding element interpolation method for analysis of thin-walled structures, Eng. Anal. Bound. Elem. 86 (2018) 82–88.
[22] G.I. Giannopoulos, N.K Anifantis, Thermal fracture interference: a two-dimensional boundary element approach, Int. J. Fract. 132 (4) (2005) 351–369.
[23] D.E. Katsareas, G.I. Giannopoulos, N.K Anifantis, A comparative study on the failure resistance of thermal barrier coatings, Comput. Struct. 84 (29–30) (2006) 1958–1964.
[24] Kuang Z.B., Ma F. S. Crack tip fields (in Chinese). Xi'an: Xi'an Jiaotong University Press; 2002.